

25 THE INTERSTELLAR MEDIUM

25.1 *Useful References*

- Choudhuri, Secs. 6.5–6.6
- Rybicki & Lightman, Sec. 10.5

25.2 *Introduction*

The **interstellar medium**, or ISM, is the nearly-empty space inside our Galaxy in which all the objects we've studied thus far are embedded (note that there is also an intergalactic medium in the spaces between galaxies).. The Milky Way is full of gas, dust, cosmic rays, and radiation, all at comparable energy densities. This forms a very complex medium, that often affects many processes involving stars and compact objects, as well as our observations of these objects.

Our focus here is on the gas and the plasma. On average, the ISM is composed of $\sim 75\%$ H and $\sim 25\%$ He, by mass. Typical densities are $n \sim 1 \text{ cm}^{-3}$ – about $100\times$ emptier than the so-called “ultra-high” vacuums found in terrestrial laboratories. The ISM is strongly inhomogeneous the material sits in various reservoirs, which are characterized using different observing techniques:

Reservoir	$n [\text{cm}^{-3}]$	$T [\text{K}]$	observed by:
H I gas (neutral)	0.3–30	30–3000	radio (typ. 21 cm)
Molecular clouds (H_2)	$\gtrsim 10^3$	30	radio
H II regions (ionized)	$0.3\text{--}10^4$	10^4	radio \rightarrow optical
Coronal gas (ionized)	~ 0.004	$\gtrsim 10^6$	radio, X-ray

The neutral species, atomic (H I) and molecular (H_2), contain most of the gas mass. Molecular clouds are where stars form, as discussed briefly in Sec. 18.1. These tend to be highly obscured, but disks and jets around young stars are often visible. H II regions require a hot, ionizing source: e.g. a white dwarf or a massive, young star. Coronal gas is blown out by supernovae.

25.3 H_2 : *Collapse and Fragmentation*

Earlier we introduced the concept of the Jeans Mass (Eq. 435), the mass required for gravitational collapse to occur,

$$M_{\text{Jeans}} = 2.3 M_{\odot} \left(\frac{T}{10 \text{ K}} \right)^{3/2} \left(\frac{n}{10^5 \text{ cm}^{-3}} \right)^{-1/2}.$$

Given the density and temperature of various stages of the ISM, we can calculate the Jeans mass in each phase:

Reservoir	$M_{\text{Jeans}}/M_{\odot}$
H I	$10^4 - 10^8$
H_2	~ 300
H II	$10^7 - 10^9$
Coronal gas	$\sim 10^{12}$

So we can see why stars form in the molecular (H_2) regions.

Once the Jeans mass has been reached and gravitational collapse sets in (see Sec .18.1), both n and T will increase in the cloud. These have competing effects: increasing n will tend to decrease the Jeans mass, while increasing T will increase the Jeans mass. If “density wins” and the net effect is a decrease in M_{Jeans} , the large collapsing cloud will then be able to collapse on much smaller scales: the cloud fragments, and the result is multiple collapsing objects. If the collapsing object can no longer easily cool, then it has likely become a protostar.

25.4 H II Regions

H II regions are zones of ionized atomic hydrogen. They are often associated with nebulae, and require gas that contains a continuous source of ionizing radiation ($h\nu > 13.6$ eV). This could be a massive star or a white dwarf, but either way it must be very hot (and so fairly young). Without that central source, the protons and electrons in the ISM will quickly recombine – even with the ionizing source, it can only ionize a region of some given volume before recombinations will be happening as quickly as ionizations. The result will be a bubble of ionized gas, termed a **Strömgen Sphere**. Such H II regions are easily observable via the strong emission lines resulting from recombination. Thus to add further to the nomenclature, they are also sometimes known as emission-line nebulae.

Our goal in the following section is to understand the size of the ionized bubble and its detailed ionization structure. In this effort, we will define the ionization fraction

$$(729) \quad f \equiv \frac{n_{\text{H}^+}(r)}{n_{\text{H}}(r)}.$$

For a fully neutral, atomic ISM $f = 0$, while full ionization implies $f = 1$. As hinted at in the preceding argument, to maintain a constant f we will want to make use of ionization equilibrium, where

$$\begin{array}{l} \text{(number of ionizing photons/sec)} \\ \text{from source} \end{array} = \begin{array}{l} \text{(number of recombinations/sec)} \\ \text{in bubble} \end{array}$$

Adopting spherical symmetry, we have

$$(730) \quad Q_* = R_{\text{recom}} \left(\frac{4}{3} \pi R^3 \right).$$

Here

$$(731) \quad Q_* \equiv \int_{\nu_m}^{\infty} \frac{L_\nu}{h\nu} d\nu$$

is the number of ionizing photons emitter per second, with $h\nu_m = 13.6$ eV. On the right-hand side, R_{recom} is the volumetric recombination rate (recombina-

tions per sec per cm^3):

$$(732) \quad R_{\text{recom}} \equiv n_p n_e \langle \sigma_{\text{recom}} v \rangle$$

$$(733) \quad = n_p n_e \alpha(T).$$

Here σ_{recom} is the free-bound cross-section for recombination. The function $\alpha(T)$ can be computed from the theory of radiative transitions; it is approximately

$$(734) \quad \alpha(T) \approx (2.6 \times 10^{-13} \text{cm}^3 \text{s}^{-1}) \left(\frac{T_{\text{gas}}}{10^4 \text{K}} \right)^{-1/2}$$

Regardless of the exact form of $\alpha(T)$, if we assume that our bubble is fully ionized (presumably with some recombinative transition zone at the edges), we will have

$$(735) \quad n_p n_e = n^2$$

and so then

$$(736) \quad Q_* = n^2 \alpha(T) \left(\frac{4}{3} \pi R^3 \right).$$

This gives the classic **Strömgen Radius** of a Strömgen sphere,

$$(737) \quad R = \left(\frac{3Q_*}{4\pi\alpha n^2} \right)^{1/3}.$$

Note that this has the expected scalings: the bubble is larger for a stronger ionizing source (larger Q_*), for a lower ambient density n , and for higher temperature T_{gas} . One can expand on this simple model a bit in a few ways. One is to consider multiple transitions in the H atoms, which gives rise to much more complicated forms for $\langle v\sigma \rangle$. Another is to require equilibrium in each of a series of nested spherical shells. In each shell, one then sets the local ionization rate (which depends on the flux reaching that radius) equal to the local recombination rate (depending on the local temperature and neutral fraction).

25.5 Plasma Waves

As noted above, much of the ISM is ionized: thus we should really treat it as a plasma, rather than a gas. This ionized mixture affects the propagation of EM radiation (especially radio waves) in several observable ways.

In what follows we focus on these propagation effects. We need to consider a dilute proton-electron plasma, possible with a background magnetic field. We will first revisit the wave equation, in order to compare it to non-vacuum wave propagation.

The wave-plasma interactions will be dominated by the electrons, because they are very light and so can respond much more quickly to changing fields. To understand how they respond, we revisit the momentum equation (Eq. 667). We have

$$(738) \quad \rho_e \left[\frac{\partial \vec{v}}{\partial t} + (\vec{v} \cdot \nabla) \vec{v} \right] = -\vec{\nabla} P - n_e e \left(\vec{E} + \frac{\vec{v}}{c} \times \vec{B} \right)$$

where \vec{v} is the velocity induced by the radiation; we'll assume this is a small value. We'll also neglect $\vec{\nabla} P$, since it is often unimportant in the ISM. Under these assumptions, and with $\rho_e = m_e n_e$, we then obtain

$$(739) \quad m_e \frac{\partial \vec{v}}{\partial t} = -e \left(\vec{E} + \frac{\vec{v}}{c} \times \vec{B} \right).$$

This is just the old Lorentz force law – which makes sense, since we're just considering changes in the electrons' momenta. Here \vec{E} comes from the EM radiation involved, whereas \vec{B} comes from whatever background \vec{B} is in the ISM. The contribution to \vec{B} from the EM radiation will be smaller by $\sim v/c$, so we ignore it.

Let's recall Maxwell's equations, specifically Faraday's Law

$$(740) \quad \vec{\nabla} \times \vec{E} = -\frac{1}{c} \frac{\partial \vec{B}}{\partial t}$$

and the Maxwell-Ampere Law

$$(741) \quad \vec{\nabla} \times \vec{B} = \frac{4\pi}{c} \vec{J} + \frac{1}{c} \frac{\partial \vec{E}}{\partial t}.$$

In our plasma,

$$(742) \quad \vec{J} = n_e (-e) \vec{v}.$$

We take the time derivative of Eq. 741, which is

$$(743) \quad \vec{\nabla} \times \frac{\partial \vec{B}}{\partial t} = \frac{4\pi}{c} \frac{\partial \vec{J}}{\partial t} + \frac{1}{c} \frac{\partial^2 \vec{E}}{\partial t^2}.$$

Taking these terms one by one, we first see that

$$(744) \quad \frac{\partial \vec{J}}{\partial t} = -n_e e \frac{\partial \vec{v}}{\partial t}$$

$$(745) \quad = \frac{n_e e^2}{m_e} \vec{E}.$$

I.e., the rate of change of the current depends on the electric field. And we can

rewrite Faraday's Law as

$$(746) \quad \frac{\partial \vec{B}}{\partial t} = -c \vec{\nabla} \times \vec{E}.$$

Thus from Maxwell's equations in a plasma we obtain

$$(747) \quad \vec{\nabla} \times \vec{\nabla} \times \vec{E} = \frac{4\pi n_e e^2}{m_e c^2} \vec{E} + \frac{1}{c^2} \frac{\partial^2 \vec{E}}{\partial t^2}.$$

To see how electromagnetic waves propagate through the plasma (and their effects on the plasma), we assume that the waves can be decomposed into a series of Fourier modes — plane waves:

$$(748) \quad \vec{E} \equiv \vec{E}_0 e^{i(\vec{k} \cdot \vec{r} - \omega t)}.$$

Applying this expression to Eq. 747, we then obtain the dispersion relation

$$(749) \quad \vec{k} \times \vec{k} \times \vec{E}_0 = \left(\frac{\omega_p^2}{c^2} - \frac{\omega^2}{c^2} \right) \vec{E}_0.$$

Here we have defined the **plasma frequency**,

$$(750) \quad \omega_p = \left(\frac{4\pi n_e e^2}{m_e} \right)^{1/2} \left(\approx 2\pi \times 10^4 \text{ Hz} \right) \left(\frac{n_e}{1 \text{ cm}^{-3}} \right)^{1/2}.$$

This dispersion relation has the character of an eigenvalue problem: an operator acting on \vec{E}_0 equals \vec{E}_0 times a constant. We can determine the velocities of each eigenmode solution via $d\omega/dk$ for each component.

We can gain further insight into this situation if we define a coordinate direction for our propagating wave:

$$(751) \quad \vec{k} = k \hat{z}.$$

This means that our wave equation (Eq. 749) now becomes

$$(752) \quad k^2 (E_y \hat{y} + E_x \hat{x}) = \frac{\omega_p^2 - \omega^2}{c^2} (E_x \hat{x} + E_y \hat{y} + E_z \hat{z})$$

which is really three equations, one for each vector component.

$$(753) \quad \begin{bmatrix} \omega_p^2 + c^2 k^2 & 0 & 0 \\ 0 & \omega_p^2 c^2 k^2 & 0 \\ 0 & 0 & \omega_p^2 \end{bmatrix} \begin{bmatrix} E_x \\ E_y \\ E_z \end{bmatrix} = \omega^2 \begin{bmatrix} E_x \\ E_y \\ E_z \end{bmatrix}$$

This has three solutions. The one along \hat{z} has the form $\omega^2 = \omega_p^2$, i.e. ω is a

constant. This is a longitudinal mode and does not propagate, since

$$(754) \quad v_{\text{group}} = \frac{d\omega}{dk} = 0.$$

The remaining two solutions lie along \hat{x} and \hat{y} . These degenerate solutions represent transverse waves and have the form

$$(755) \quad \omega^2 = c^2 k^2 + \omega_p^2$$

and so have nonzero velocities

$$(756)$$

$$v_{\text{group}} = \frac{d\omega}{dk} = \frac{c^2 k}{\omega}$$

$$(757)$$

$$= c \left(1 + \frac{\omega_p^2}{c^2 k^2} \right)^{-1/2}$$

$$(758)$$

$$= c \left(1 - \frac{\omega_p^2}{\omega^2} \right)^{+1/2}$$

The longitudinal modes are **plasma modes**: non-propagating disturbances in the plasma, indicating local bunching and rarefactions (i.e., density fluctuations). The electric field then sets up a restoring force, as sketched schematically in Fig. 61. If charge carriers in a neutral block of gas with volume $A\Delta x$ are separated, a plane-parallel electric field will be set up with

$$(759) \quad E = 4\pi\sigma = \frac{4\pi n_e e A \Delta x}{A}.$$

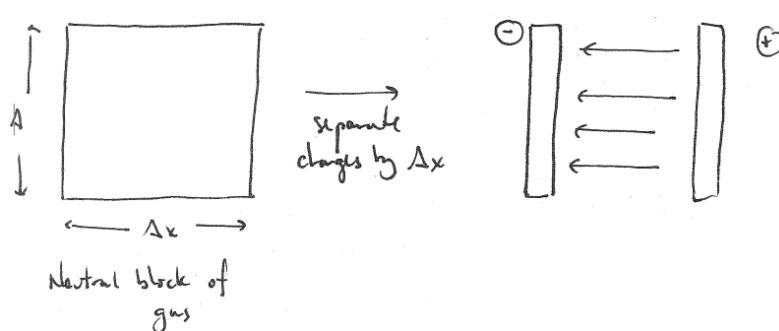


Figure 61: Intuitive picture: charges are separated in a neutral block of gas (left), setting up an electric field (right) which itself sets up a restoring force.

The restoring force on the charge carriers will then be

$$(760) F = m_e \frac{d^2 \Delta x}{dt^2} = -eE$$

and so

$$(761) \frac{d^2 \Delta x}{dt^2} + \frac{4\pi n_e e^2}{m_e} \Delta x = 0$$

$$(762) \frac{d^2 \Delta x}{dt^2} + \omega_p^2 \Delta x = 0.$$

So in plasma modes, when charges are initially perturbed they will subsequently oscillate with frequency ω_p (Eq. 750).

Fig. 62 shows the dispersion relation $\omega(k)$. The frequency ω has its minimum value at $\omega(k = 0) = \omega_p$ and increases with $|k|$. Thus, modes with $\omega < \omega_p$ cannot propagate through the ISM.

Plasma modes play an important role in both the ISM as well as closer to home, in the Earth's ionosphere.

Medium	n_e [cm ⁻³]	f_p [Hz]	λ_p
ISM	~ 0.03	1700	180 km
ionosphere	$\sim 10^5$	3×10^6	100 m

The ionospheric cutoff means that radio waves with $\lambda \gtrsim 100$ m cannot propagate through the Earth's atmosphere: ground-based radio astronomy is impossible at these frequencies! On the other hand, the same argument holds for terrestrial radio emissions: they are blocked from reaching space, but can instead be reflected beyond direct line-of-sight and far around the globe.

As a final note, solid metals look very much like a free electron gas to incident photons. In this case, the characteristic $\lambda_p \sim 10$ s of nm and longer-wavelength radiation cannot propagate through the metal. Thus solid metals reflect visible light, but are (largely) transparent to high-energy UV and X-ray

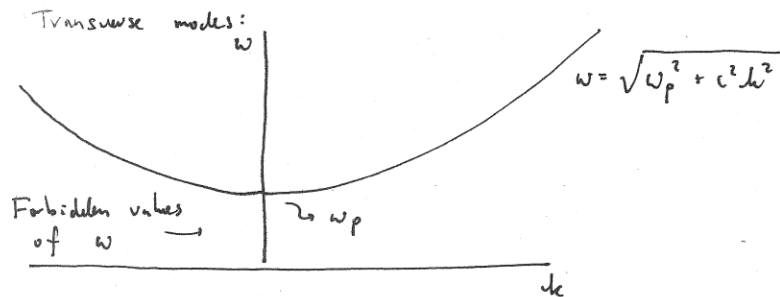


Figure 62: Dispersion relation for transverse plasma modes. Modes with $\omega < \omega_p$ cannot propagate.

radiation.

25.6 Waves in the ISM

Some of the most-observed radio sources embedded in the ISM are pulsars (though there are many others). Each emitted pulse travels through the ISM, and its wave speed will be affected by its propagation through the plasma. If it is a distance d away, the travel time of the pulse is

(763)

$$t_{\text{pulse}} = \int_0^d \frac{d\ell}{v_{\text{group}}}$$

(764)

$$= \frac{1}{c} \int_0^d \left(1 - \frac{\omega_p^2}{\omega^2}\right)^{-1/2} d\ell.$$

If we are observing at fairly high frequencies compared to the ISM's cutoff frequency (just ~ 2 kHz) then we can simplify this somewhat as

(765)

$$t_{\text{pulse}} \approx \frac{d}{c} + \frac{1}{c} \int_0^d \frac{\omega_p^2}{2\omega^2} d\ell$$

(766)

$$= \frac{d}{c} + \frac{2\pi e^2}{m_e c \omega^2} \int_0^d n_e d\ell$$

We don't know when the pulse was actually emitted, so a measurement at a single frequency won't help us much. But we can look at the offset in the time of arrival as a function of frequency (or wavelength):

(767)

$$\frac{dt_p}{d\omega} = -\frac{4\pi e^2}{m c \omega^3} \int_0^d n_e d\ell$$

(768)

$$= -\frac{4\pi e^2}{m c \omega^3} \langle n_e \rangle d.$$

The initial fraction is just a set of physical or observed constants; the remaining quantities are defined as the **Dispersion Measure**

(769) $DM = \langle n_e \rangle d.$

Using sources with known distances, we have established that $\langle n_e \rangle \approx 0.03 \text{ cm}^{-3}$

in most areas of the Milky Way. We can then measure $dt_p/d\omega$ to directly estimate the distances to pulsars!

We can also examine the propagation of waves through the ISM in the presence of a time-changing \vec{B} (which we have ignored up to now). The calculation is not trivial! But the key, final result is that right-hand and left-hand circular polarization states will travel at different speeds:

$$(770) \quad k_{L/R} = \frac{\omega}{c} \left(1 - \frac{\omega_p}{\omega(\omega \pm \omega_c)} \right)^{1/2}$$

where

$$(771) \quad \omega_c \equiv \frac{eB_{\parallel}}{m_e c}$$

and

$$(772) \quad B_{\parallel} = \vec{B} \cdot \vec{k}/k.$$

Since any linearly-polarized wave can be regarded as the combination of two circular polarizations, any linearly-polarized plane wave will see its direction of polarization rotate as the two circular waves move at different speeds. We see

$$(773) \quad \Delta\theta_p = \int_0^d \frac{k_L - k_R}{2} dz \equiv \text{RM} \lambda^2$$

where RM is the observed **Rotation Measure**. Observationally we again look at how this changes with frequency:

$$(774) \quad \frac{d\theta}{d\omega} = -\frac{1}{\omega^3} \frac{4\pi e^3}{m_e^2 c^2} \int_0^d n_e B_{\parallel} dz.$$

This gives us a way to infer magnetic field strengths throughout the ISM, just using radio wave observations (and a bit of astrophysics).